

Failure of Time-Dependent Density Functional Theory for Long-Range Charge-Transfer Excited States: The Zincbacteriochlorin–Bacteriochlorin and Bacteriochlorophyll–Spheroidene Complexes

Andreas Dreuw*[†] and Martin Head-Gordon[‡]

Contribution from the Institut für Physikalische und Theoretische Chemie, Johann Wolfgang Goethe-Universität Frankfurt, Marie-Curie-Strasse 11, 60439 Frankfurt, Germany, and Department of Chemistry, University of California, Berkeley, and Chemical Science and Physical Bioscience Division, Lawrence Berkeley National Laboratory, Berkeley, California 94720-1470

Received November 12, 2003; E-mail: andreas.dreuw@theochem.uni-frankfurt.de

Abstract: It is well-known that time-dependent density functional theory (TDDFT) yields substantial errors for the excitation energies of charge-transfer (CT) excited states, when approximate standard exchange-correlation (xc) functionals are used, for example, SVWN, BLYP, or B3LYP. Also, the correct $1/r$ asymptotic behavior of CT states with respect to a distance coordinate R between the separated charges of the CT state is not reproduced by TDDFT employing these xc-functionals. Here, we demonstrate by analysis of the TDDFT equations that the first failure is due to the self-interaction error in the orbital energies from the ground-state DFT calculation, while the latter is a similar self-interaction error in TDDFT arising through the electron transfer in the CT state. Possible correction schemes, such as inclusion of exact Hartree–Fock or exact Kohn–Sham exchange, as well as aspects of the exact xc-functional are discussed in this context. Furthermore, a practical approach is proposed which combines the benefits of TDDFT and configuration interaction singles (CIS) and which does not suffer from electron-transfer self-interaction. The latter approach is applied to a (1,4)-phenylene-linked zincbacteriochlorin–bacteriochlorin complex and to a bacteriochlorophyll–spheroidene complex, in which CT states may play important roles in energy and electron-transfer processes. The errors of TDDFT alone for the CT states are demonstrated, and reasonable estimates for the true excitation energies of these states are given.

1. Introduction

Time-dependent density functional theory (TDDFT)^{1,2} has become one of the most popular quantum chemical approaches for calculating electronic spectra of medium-sized and large molecules up to 200 second-row atoms (see, for example, refs 3–6). Although TDDFT reaches the accuracy of sophisticated quantum chemical methods for valence-excited states, which are energetically well below the first ionization potential, its computational cost is remarkably low. In present-day TDDFT, one relies on the so-called adiabatic approximation,^{1,2} and approximate ground-state exchange-correlation (xc) functionals are applied.^{7–10}

One major drawback of these approximate xc-functionals is that the corresponding potentials do not exhibit the correct $1/r$ asymptotic behavior, where r is the electron–nucleus distance,¹¹ but fall off too rapidly.¹² Also, for many xc-functionals, the corresponding xc-potential is too high in the inner regions, resulting in underbound virtual orbitals.^{11,13} This leads, for instance, to substantial errors for the excitation energies of Rydberg states in which the electron travels far away from the nucleus. Today, it is known that this failure can be compensated by using asymptotically corrected potentials such as LB94.¹⁴ However, it has been pointed out recently that TDDFT also gives substantial errors for excited states of molecules with extended π -systems^{15,16} as well as for charge-transfer (CT) states.^{6,17,18} Especially, excitation energies of long-range CT states in weakly interacting molecular complexes are drastically

[†] Johann Wolfgang Goethe-Universität Frankfurt.

[‡] University of California, Berkeley and Lawrence Berkeley National Laboratory.

- (1) Casida, M. E. In *Recent Advances in Density Functional Methods, Part I*; Chong, D. P., Ed.; World Scientific: Singapore, 1995.
- (2) Gross, E. U. K.; Dobson, J. F.; Petersilka, M. In *Density Functional Theory II*; Nalewajski, R. F., Ed.; Springer: Heidelberg, 1996.
- (3) Sundholm, D. *Chem. Phys. Lett.* **1999**, *302*, 480.
- (4) Furche, F.; Ahlrichs, R.; Wachsmann, C.; Weber, E.; Sobanski, A.; Vogtle, F.; Grimme, S. *J. Am. Chem. Soc.* **2000**, *122*, 1717.
- (5) Dreuw, A.; Dunietz, B. D.; Head-Gordon, M. *J. Am. Chem. Soc.* **2002**, *124*, 12070.
- (6) Dreuw, A.; Fleming, G. R.; Head-Gordon, M. *J. Phys. Chem. B* **2003**, *107*, 6500.
- (7) Dirac, P. A. M. *Proc. Cambridge Philos. Soc.* **1930**, *26*, 376.

- (8) Vosko, S. H.; Wilk, L.; Nusair, M. *Can. J. Phys.* **1980**, *58*, 1200.
- (9) Becke, A. D. *Phys. Rev. A* **1988**, *38*, 3098.
- (10) Becke, A. D. *J. Chem. Phys.* **1993**, *98*, 5648.
- (11) Casida, M. E.; Jamorski, C.; Casida, K. C.; Salahub, D. R. *J. Chem. Phys.* **1998**, *108*, 4439.
- (12) Tozer, D. J.; Handy, N. C. *J. Chem. Phys.* **1998**, *109*, 10180.
- (13) Casida, M. E.; Casida, K. C.; Salahub, D. R. *Int. J. Quantum Chem.* **1998**, *70*, 933.
- (14) van Leeuwen, R.; Baerends, E. J. *Phys. Rev. A* **1994**, *49*, 2421.
- (15) Cai, Z.-L.; Sendt, K.; Reimers, J. R. *J. Chem. Phys.* **2002**, *117*, 5543.
- (16) Grimme, S.; Parac, M. *ChemPhysChem* **2003**, *3*, 292.

underestimated, and the potential energy curves of these states do not exhibit the correct $1/R$ asymptotic behavior, where R is a distance coordinate between the separated charges of the CT state.^{6,19} In recent work,^{18,20} it has been shown that the latter failure of TDDFT employing standard ground-state xc-functionals can be traced back to the lack of exact nonlocal Hartree–Fock (HF) exchange. In linear response theory, the electrostatic interaction between the positive and negative charges within the CT state is contained in the response of the HF exchange term. In this work, we will demonstrate that the failure of TDDFT for CT states can in fact be understood as a self-interaction error.

Despite its failure for CT states, TDDFT has recently been applied to several molecular complexes of biological relevance, in which long-range CT states might be relevant. For example, phenylene-linked free-base porphyrin and zincporphyrin complexes as well as their bacteriochlorin (BC) analogues have been investigated.^{21,22} These complexes constitute important model systems mimicking the function of photosynthetic arrays of chlorophylls as they are present in light-harvesting complexes of plants and purple bacteria.^{23–25} Naturally, the understanding of how the linking of chromophores modifies the structural and electronic properties of the components is crucial for the design of artificial arrays of chromophores suitable for solar energy conversion schemes. Unfortunately, a plethora of spurious CT states was obtained in the visible range of the spectra of these compounds when TDDFT with a standard ground-state xc-functional was applied.^{21,22} On the contrary, in a similar study of linked zincporphyrin dimers in which the symmetry adapted cluster configuration interaction (SAC-CI) method has been employed, CT states were not found in the energy regime of the energetically lowest Q states of zincporphyrins,²⁶ which is in accordance with experimental findings (see ref 27 and references therein). Another example for an application of TDDFT to biological systems is the calculation of the excited states of a bacteriochlorophyll–spheroidene (BChl–Spher) complex.²⁸ The knowledge of the energetic position of the excited states of the complex is important for the fundamental understanding of the excitation-energy transfer processes in the light-harvesting complex LH2 of purple bacteria. Employing TDDFT with the standard hybrid B3LYP xc-functional yields also in this case three artificially low-lying CT states, all of them well below the first valence-excited Q_y band of the bacteriochlorophyll molecule.²⁸ We will show that this is also

an artifact of TDDFT employing approximate xc-functionals. Such calculations can have a strong impact on the interpretation of experimental results and can lead to a complete misunderstanding of the underlying physical mechanisms.

The aim of this work is two-fold. First, in section 2, the failure of TDDFT for CT states will be theoretically analyzed in detail, and it will be shown how this failure can be understood as electron-transfer self-interaction error. Furthermore, we suggest a practical approach to work around this CT problem based on the combination of TDDFT and configuration interaction singles (CIS).²⁹ After outlining the details of our computations in section 3, we demonstrate the failure of TDDFT for CT states at hand for two examples, a phenylene-linked zincbacteriochlorin–bacteriochlorin complex (section 4.1) and a bacteriochlorophyll–spheroidene complex (section 4.2). It will be shown that the previously obtained energetically low-lying CT states are artifacts of TDDFT. Employing a hybrid approach of TDDFT and CIS, the excited states of the complexes are reinvestigated, and their relevance in biological processes is reevaluated.

2. Charge-Transfer States in TDDFT

As already mentioned in the Introduction, it has been observed several times that TDDFT yields substantial errors for excitation energies of charge-transfer excited states.^{6,17–20} The excitation energies for such states are usually drastically underestimated, and the potential energy curves of CT states do not exhibit the correct $1/R$ dependence along a charge-separation coordinate R ,²⁰ although in reality the positive and negative charges in a CT state electrostatically attract each other, and, thus, separating these charges must have an attractive $1/R$ dependence. These failures of TDDFT in the calculation of CT states can be understood by analyzing the basic equations. For real Kohn–Sham orbitals, the TDDFT scheme is a non-Hermitian eigenvalue problem of the form

$$\begin{pmatrix} \mathbf{A} & \mathbf{B} \\ \mathbf{B} & \mathbf{A} \end{pmatrix} \begin{pmatrix} \mathbf{X} \\ \mathbf{Y} \end{pmatrix} = \omega \begin{pmatrix} 1 & 0 \\ 0 & -1 \end{pmatrix} \begin{pmatrix} \mathbf{X} \\ \mathbf{Y} \end{pmatrix} \quad (1)$$

If a general hybrid functional is applied, that is, one that contains also parts of HF exchange, the elements of the matrices \mathbf{A} and \mathbf{B} can be formally written (in the canonical basis) as

$$\begin{aligned} A_{ia\sigma,jb\tau} &= \delta_{\sigma\tau} \delta_{ij} \delta_{ab} (\epsilon_{a\sigma} - \epsilon_{i\tau}) \\ &+ (i_{\sigma} a_{\sigma} | j_{\tau} b_{\tau}) - \delta_{\sigma\tau} c_{\text{HF}} (i_{\sigma} j_{\sigma} | a_{\tau} b_{\tau}) \\ &+ (1 - c_{\text{HF}}) (i_{\sigma} a_{\sigma} | f_{\sigma\tau} | j_{\tau} b_{\tau}) \end{aligned} \quad (2)$$

$$\begin{aligned} B_{ia\sigma,jb\tau} &= (i_{\sigma} a_{\sigma} | b_{\tau} j_{\tau}) - \delta_{\sigma\tau} c_{\text{HF}} (i_{\sigma} b_{\sigma} | a_{\tau} j_{\tau}) \\ &+ (1 - c_{\text{HF}}) (i_{\sigma} a_{\sigma} | f_{\sigma\tau} | b_{\tau} j_{\tau}) \end{aligned} \quad (3)$$

where ij are used for ground-state occupied orbitals, a, b are used for virtual orbitals, and σ and τ are the spin variables. The four-index integrals are written in the typical Mulliken notation. ϵ refers to the ground-state orbital energy, and c_{HF} is the coefficient of the HF exchange part in the hybrid functionals. In this form, eqs 2 and 3 contain pure TDDFT as well as time-dependent Hartree–Fock (TDHF) as limiting cases when $c_{\text{HF}} = 0$ or $c_{\text{HF}} = 1$, respectively. The last terms of eqs 2 and 3 are in the adiabatic approximation defined as

- (17) Tozer, D. J.; Amos, R. D.; Handy, N. C.; Roos, B. J.; Serrano-Andres, L. *Mol. Phys.* **1999**, *97*, 859.
 (18) Sobolewski, A. L.; Domcke, W. *Chem. Phys.* **2003**, *294*, 73.
 (19) Dreuw, A.; Fleming, G. R.; Head-Gordon, M. *Phys. Chem. Chem. Phys.* **2003**, *5*, 3247.
 (20) Dreuw, A.; Weisman, J. L.; Head-Gordon, M. *J. Chem. Phys.* **2003**, *119*, 2943.
 (21) Yamaguchi, Y.; Yokomichi, Y.; Yokoyama, S.; Mashiko, S. *Int. J. Quantum Chem.* **2001**, *84*, 338.
 (22) Yamaguchi, Y.; Yokoyama, S.; Mashiko, S. *J. Chem. Phys.* **2002**, *116*, 6541.
 (23) Miyatake, T.; Timiaki, H.; Holzwarth, A. R.; Schaffner, K. *Plant Physiol.* **2001**, *125*, 1558.
 (24) Burrell, A. K.; Officer, D. L.; Reid, D. C. W.; Scott, S. M.; Gordon, K. C. *J. Porphyrins Phthalocyanines* **2000**, *4*, 627.
 (25) Balzani, V.; Juris, A.; Venturi, M. *Chem. Rev.* **1996**, *96*, 759.
 (26) Miyahara, T.; Nakatsui, H.; Hasegawa, J.; Osuka, A.; Aratani, N.; Tsuda, A. *J. Chem. Phys.* **2002**, *117*, 11196.
 (27) Cho, H. S.; Jeong, D. H.; Yoon, M.-C.; Kim, Y. H.; Kim, Y.-R.; Kim, D.; Jeoung, S. C.; Kim, S. K.; Aratani, N.; Shinmori, H.; Osuka, A. *J. Phys. Chem. A* **2001**, *105*, 4200.
 (28) Polivka, T.; Zigmantas, D.; Herek, J. L.; He, Z.; Pascher, T.; Pulleritis, T.; Cogdell, R. J.; Frank, H. A.; Sundström, V. *J. Phys. Chem. B* **2002**, *106*, 11016.

- (29) del Bene, J.; Ditchfield, R.; Pople, J. A. *J. Chem. Phys.* **1971**, *55*, 2236.

$$(i_{\sigma}a_{\sigma}|f_{\sigma\tau}|j_{\tau}b_{\tau}) = \int \int \phi_i(r_1)\phi_a(r_1)f_{\sigma\tau}(r_1, r_2)\phi_j(r_2)\phi_b(r_2) dr_1 dr_2 \quad (4)$$

where $f_{\sigma\tau}(r_1, r_2)$ is the time-independent nonlocal xc-kernel. The kernel is usually further approximated by using local xc-functionals resulting in the adiabatic local-density approximation (ALDA). The explicit form is given, for example, in ref 30 and requires that $f_{\sigma\tau}(r_1, r_2) \rightarrow f_{\sigma\tau}(r_1)\delta(r_1 - r_2)$.

In contrast to a valence-excited state, in an intermolecular charge-transfer state an electron is in general transferred from an occupied orbital i of molecule A to a virtual orbital a of another molecule B (Figure 1). For simplicity, let us assume that the overlap between orbitals on molecule A and orbitals on molecule B is zero. For such a CT state, the first term of eq 2 yields the difference of the energies of the donor orbital i on A and the acceptor orbital a on B. The second term corresponding to the response of the Coulomb part of the Kohn–Sham operator has the appearance of an exchange term and is zero, because the orbitals i on A and a on B do not overlap. The third term of eq 2 originates from the nonlocal HF exchange part of the Kohn–Sham operator; that is, it is its linear response. This term contributes to the matrix elements of **A**, because orbitals i and j are both on A and the orbitals a and b are on B. In fact, this term is a Coulomb term, because the created holes (orbitals i and j) interact with the electrons (orbitals a and b), which relates to the electrostatic attraction within the CT state. Consequently, this term is essential for the correct $1/R$ dependence of the potential energy curves of CT states along the intermolecular separation coordinate. Going to the fourth term, which is the response of the xc-potential, it does not contribute to the matrix element, when an approximate xc-functional is used, again, because the overlap between a and i is zero. The same arguments are valid for the elements of matrix **B** (eq 3), and all terms are zero as well; that is, this matrix does not contribute to CT states at all. For CT states, eqs 2 and 3 reduce to the following simple expressions

$$A_{i\sigma,jb\tau} = \delta_{\sigma\tau}\delta_{ij}\delta_{ab}(\epsilon_{a\sigma} - \epsilon_{i\tau}) - \delta_{\sigma\tau}c_{\text{HF}}(i_{\sigma}j_{\sigma}|a_{\tau}b_{\tau}) \quad (5)$$

$$B_{i\sigma,jb\tau} = 0 \quad (6)$$

When a pure local xc-functional (SVWN, BLYP,⁹ or LB94) is employed, that is, $c_{\text{HF}} = 0$, the excitation energy of a CT state in TDDFT is simply given by the difference of the orbital energies of the electron-accepting and electron-donating molecular orbitals ϵ_a and ϵ_i , respectively. Within HF theory, this is already a rough estimate for the energy of the CT state at large distances, because Koopman's theorem states that $-\epsilon_i$ and $-\epsilon_a$ correspond to the ionization potential of molecule A and to the electron affinity of molecule B, respectively. This is due to the fact that the occupied orbitals are calculated for the N electron system while the virtual orbitals are formally evaluated for the $N + 1$ electron system. This is not the case in density functional theory following the Kohn–Sham formalism (DFT), because the same potential is used to calculate the occupied and virtual orbitals. As a consequence, while the HOMO still corresponds to the IP, the LUMO is generally more strongly bound in DFT than in HF theory and cannot be related to the EA. Because the negative of the LUMO energy is therefore

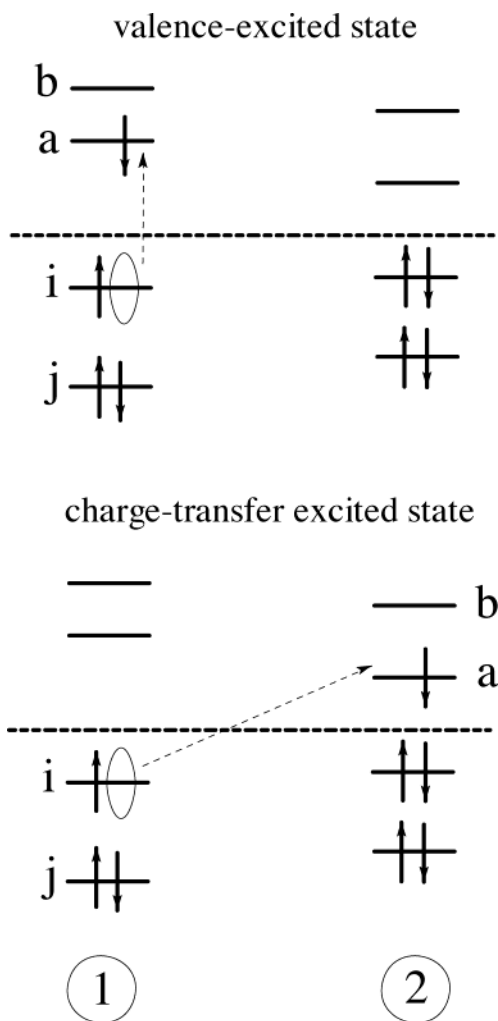


Figure 1. Schematic sketch of a typical valence-excited state, in which the transition occurs on one of the individual molecules; that is, the orbitals i , j , a , and b are located on the same molecule as compared to a charge-transfer excited state in which an electron is transferred from orbital i on molecule 1 to orbital a on molecule 2. When molecules 1 and 2 are spatially separated from each other, the orbitals i and j do not overlap with a and b .

much larger than the true EA, the orbital energy difference corresponding to a CT state is usually a drastic underestimation of its correct excitation energy.

The orbital energies stemming from a DFT calculation also suffer from the so-called self-interaction (SI), which arises from the fact that the Coulomb interaction with all occupied orbitals is contained in the orbital energy, including the interaction with the orbital under consideration itself. In Hartree–Fock theory, this is not a problem, because exact exchange guarantees an exact cancellation of the artificially introduced error. However, in DFT, the HF exchange potential is replaced by an approximate xc-potential which does not cancel the self-interaction error in the Coulomb part correctly. Because the SI error is of the same order of magnitude for the occupied and virtual orbitals, the orbital energy differences are usually good approximations for excitation energies of non-CT states, which do not require a change in electron numbers on independent subsystems. In large part, this is why TDDFT is quite accurate for non-CT valence-excited states.

Because the excitation energy of a CT state is simply given by the constant difference of the energies of the electron-

(30) Hirata, S.; Head-Gordon, M. *Chem. Phys. Lett.* **1999**, *302*, 375.

donating and electron-accepting orbitals when a pure xc-functional is employed, the potential energy curves of CT states do not exhibit the correct $1/R$ shape along a distance coordinate. As already mentioned, the electrostatic attraction between the positive charge (the holes i, j on A) and the negative charge (the electrons a, b on B) is contained in the second term of eq 5, which corresponds to the linear response of HF exchange. Therefore, the correct $1/R$ long-range behavior of the potential energy surfaces can in fact be obtained when nonlocal HF exchange is used as xc-potential. Including exact HF exchange by using hybrid functionals improves the asymptotic behavior according to the factor c_{HF} of the exchange functional, because the second term of eq 5 depends linearly on c_{HF} . This explains the previously observed asymptotic behavior of potential energy curves of CT states of a tetrafluoroethylene–ethylene complex calculated with the SVWN, LB94, B3LYP, and “half-and-half” functional as compared to configuration interaction singles (CIS).²⁰

The $1/R$ failure of TDDFT employing pure standard xc-functionals can in fact be understood as a self-interaction error. To illuminate this, let us first inspect the case of TDHF ($c_{\text{HF}} = 1$ in eq 5). The excitation energy of a long-range CT state, where an electron is excited from orbital i on molecule A into orbital a on molecule B, is dominated by the orbital energy difference $\epsilon_a - \epsilon_i$. In general, ϵ_a contains the Coulomb repulsion of orbital a with all occupied orbitals of the ground state including the orbital i , which is no longer occupied in the CT state. In other words, the electrostatic repulsion between orbital a and i , the integral $(aa|ii)$, is contained in the orbital energy difference, although orbital i is empty in the CT state. That means that the transferred electron in orbital a experiences the electrostatic repulsion with itself still being in orbital i ; in other words, it experiences molecule A as neutral. This electron-transfer self-interaction effect is canceled in TDHF by the response of the HF exchange term, the second term of eq 5, being $(ii|aa)$, which gives rise to the particle–hole attraction. In pure TDDFT employing approximate xc-functionals, HF exchange is not present and the electron-transfer self-interaction effect is not exactly canceled, leading to an incorrect long-range behavior of their potential energy curves.

However, if the exact Kohn–Sham xc-potential would be used, which unfortunately is not known, the correct $1/R$ long-range behavior would be found. This is due to the derivative discontinuities of the exact exchange–correlation energy with respect to particle number.³¹ In the case of an electron transfer from orbital i of molecule A to orbital a of molecule B, the xc-potential jumps discontinuously by the constant $\text{IP}_A - \text{EA}_B$, leading to a singularity in the derivative of the potential with respect to the density, that is, the xc-kernel f_{xc} used in the TDDFT calculation (eqs 2 and 3). This singularity then compensates the overlap between the orbitals i and a which approaches zero when the molecules A and B are being separated, and, thus, the fourth term of eq 2 does in fact contribute to a CT state when the exact xc-potential would be employed. The correct $1/R$ asymptote along the separation coordinate would then be obtained for a CT state. Furthermore, this clearly explains why standard approximate xc-functionals in TDDFT fail in describing long-range CT states correctly

because they do not contain the derivative discontinuities. Optimized effective potentials (OEPs) which correspond to exact local exchange potentials have recently been introduced by Görling³² and Ivanov et al.³³ and may be able to yield the correct asymptotic $1/R$ dependence of excited CT states, because they possess singularities as soon as the overlap between the electron-donating and electron-accepting orbitals i and a , respectively, approaches zero. This, however, remains to be explored in detail, and it seems numerically demanding to compensate the convergence of the overlap toward zero with the convergence of the xc-kernel f_{xc} to infinity such that the fourth term of eq 2 cancels the electron-transfer self-interaction error correctly and recovers the correct $1/R$ asymptote.

It is also worthwhile to note that the \mathbf{B} matrix (eq 3) vanishes for a long-range CT state. Because the neglect of the \mathbf{B} matrix is equivalent to applying the Tamm–Dancoff approximation, which in the case of TDHF yields CIS, both methods give identical results for the energies of long-range CT states. The same is true for TDDFT as compared to its Tamm–Dancoff approximation TDA/TDDFT.³⁴

In summary, TDDFT yields fairly accurate results for valence-excited states but fails in describing CT states. The excitation energies are severely too low, and the potential energy curves do not exhibit the correct $1/R$ asymptote. In contrast to TDDFT methods, CIS and TDHF yield the correct $1/R$ behavior of the potential energy curves of CT states with regard to a distance coordinate, because of the full inclusion of HF exchange, which leads to the cancellation of electron-transfer self-interaction. On the other hand, the excitation energies calculated with CIS or TDHF are usually much too large because of the lack of dynamical correlation. Therefore, we suggest the use of a hybrid scheme that combines the benefits of both methods to obtain reasonable estimates for the energies and potential energy surfaces of CT states relative to valence-excited states. This approach should only be seen as a practical work-around to the CT problem in TDDFT until a theoretically sounder solution is found. However, it is a useful “diagnostic” for whether CT states are in the range of the valence excitations of interest.

As the first step of this hybrid approach, a ground-state DFT calculation is performed for the energetically lowest CT state at a large intermolecular distance (R_0) by exchanging the orbital i located at molecule A against the orbital a located at molecule B in the β -part of the wave function. To converge the DFT calculation onto the energetically lowest CT state, we generally use the geometric direct minimization technique (GDM).³⁵ At shorter distances when the orbitals start to overlap, GDM converges to the closed-shell ground state of the dimer, presumably because the CT solution is no longer a distinct wave function minimum. Otherwise, this would provide a convenient way to map out a complete potential energy surface of the CT state. A corrected excitation energy for the lowest CT state is then easily obtained by subtraction of the total energies of the ground state and the CT state, which corresponds to the known Δ DFT method.³⁶ This excitation energy does not suffer from electron-transfer self-interaction. The self-interaction free long-range value of the CT excitation energy is then used as a

(32) Görling, A. *Phys. Rev. Lett.* **1999**, *83*, 5459.

(33) Ivanov, S.; Hirata, S.; Bartlett, R. J. *Phys. Rev. Lett.* **1999**, *83*, 5455.

(34) Hirata, S.; Head-Gordon, M. *Chem. Phys. Lett.* **1999**, *314*, 291.

(35) Voorhis, T. V.; Head-Gordon, M. *Mol. Phys.* **2002**, *100*, 1713.

(36) Ziegler, T.; Rauk, A.; Baerends, E. J. *Theor. Chim. Acta* **1977**, *43*, 261.

(31) Perdew, J. P.; Parr, R. G.; Levy, M.; Balduz, J. L., Jr. *Phys. Rev. Lett.* **1982**, *49*, 1691.

constant offset (for exchange-correlation effects) for the asymptotically correct potential energy curve calculated at the CIS level:

$$\omega_{\text{CT}}(R) = \omega_{\text{CT}}^{\text{CIS}}(R) + (\Delta\text{DFT}(R_0) - \omega_{\text{CT}}^{\text{CIS}}(R_0)) \quad (7)$$

The quality of the total energy of the CT state is roughly the same as that of the ground state, because the energetically lowest CT state usually corresponds to a pure occupied-virtual single-electron transition over the considered distance range; that is, the excited state is well described by a single Slater determinant. Furthermore, in the limit of the exact xc-functional, TDDFT and ΔDFT are equivalent. Plotting the shifted CIS curve together with the curves of the valence-excited states calculated with TDDFT yields a complete self-interaction free picture of all relevant excited states of the dimer. We have investigated the error that is introduced by using the CIS curve instead of the ΔDFT curve by studying the energetically lowest CT state of a tetrafluoroethylene–ethylene dimer. In this small system, it is possible to converge the ground-state DFT calculation at even shorter distances onto the CT state with the help of a maximum-overlap-method (MOM)³⁷ and thereby to map out a complete potential energy surface for the CT state. We found that, by using the CIS curve with the self-interaction free offset value instead of the ΔSCF curve, one introduces an additional error of at most 0.1 eV. Therefore, it can be expected that the accuracy of the hybrid approach for CT states is of about the same order as TDDFT is for valence-excited states.

The proposed hybrid approach is of course not useful for small systems, because more reliable wave function-based methods are available, but for large systems, however, this approach is at present the only possibility for gaining insight into the energetic positions of intermolecular CT states as compared to valence-excited states and for obtaining reasonable potential energy curves along an intermolecular separation coordinate. The computational cost of the hybrid approach is about double that of TDDFT or CIS alone, because one needs to run both methods of similar cost independently. The hybrid approach has already been successfully applied to CT states in large xanthophyll–chlorophyll dimers.^{6,19} In the following sections, this approach will be used to gain insight into the energetic location of intermolecular CT states in zincbacteriochlorin–bacteriochlorin (ZnBC–BC) and bacteriochlorophyll–spheroidene (BChl–Spher) complexes.

3. Computational Details

Our theoretical investigation comprises the optimization of the geometries of the species applying the Kohn–Sham density functional theory (DFT)^{38–40} and the calculation of their excited states with the time-dependent-density functional theory (TDDFT)^{1,2} as well as with the above-described hybrid approach between TDDFT and configuration interaction singles (CIS). The details of our calculations for the ZnBC–BC and the bacteriochlorophyll–spheroidene complexes will be outlined in the following two paragraphs. All calculations have been performed in the framework of the Q-Chem package of programs.⁴¹

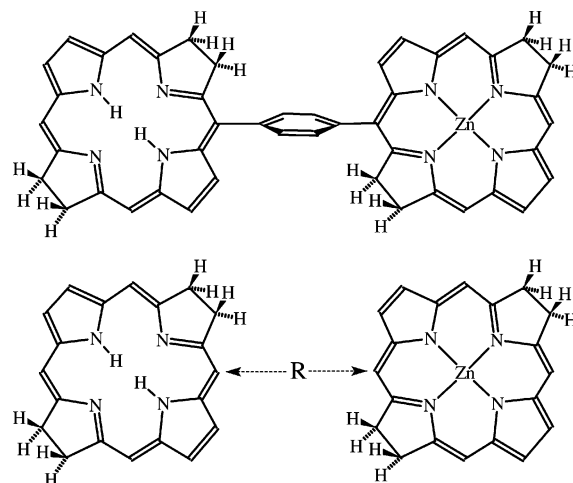


Figure 2. Molecular structure of the (1,4)-phenylene-linked zincbacteriochlorin–bacteriochlorin complex as well as of the model complex used in some calculations. The distance coordinate R is here defined as the distance between the formerly linked carbon atoms.

3.1. Zincbacteriochlorin–Chlorin Complex. The structures of the monomers ZnBC and free-base BC as well as the structure of the phenylene-linked complex ZnBC–BC (Figure 2) have been optimized at the level of DFT employing the hybrid B3LYP¹⁰ xc-functional and the 6-31G* basis set, which is known to yield reliable ground-state geometries. Based on these geometries, the excited states of the monomers and the complex have been calculated employing TDDFT with the BLYP⁹ xc-functional and the 6-31G* basis set. We have chosen the same xc-functional as Yamaguchi et al.²² because they have already shown that this functional and basis set combination yields reasonable results for the low-lying electronic states of the monomers and because it allows for direct comparison of our results with theirs. Because TDDFT yields energetically too low intermolecular CT states in the investigated complex, we have also used the suggested hybrid approach combining TDDFT/BLYP/6-31G* and CIS/6-31G* to calculate the excited states of the dimer along an intermolecular distance coordinate R as defined in Figure 2. For these calculations, we used a model complex in which the phenylene-linkage is neglected. As will be shown later in detail, the differences between the excited states calculated for the full complex and those for the model complex are very small.

3.2. Bacteriochlorophyll–Spheroidene Complex. For the calculations of the excited states of the B800' bacteriochlorophyll–spheroidene complex, the crystal structure of the LH2 complex of *Rhodospseudomonas acidophila* was used.⁴² The positions of the hydrogen atoms and of the carbon atoms of the conjugated chain of spheroidene have been reoptimized using DFT/B3LYP/6-31G*, because the accuracy of the crystal structure is not sufficient. In particular, the correct conjugation scheme of spheroidene can have a significant influence on the energetic position of the excited states of the carotenoid. The positions of all other atoms were held fixed during the reoptimization. The excited states of the optimized complex have been calculated employing the Tamm–Dancoff approximation to TDDFT, TDA/TDDFT,³⁴ in combination with the BLYP xc-functional and the 3-21G basis set. It has been shown previously that TDA/TDDFT yields good results for the excited states of tetrapyrrols as well as for carotenoids.^{6,19,43,44} In particular, the low-lying excited states of carotenoids, which are the dipole-forbidden S_1 and the strongly allowed S_2 state, are given in the

(37) Gilbert, A. T. B.; Gill, G. B. W.; Gill, P. M. W., in preparation.

(38) Hohenberg, P.; Kohn, W. *Phys. Rev.* **1964**, *136*, B864.

(39) Kohn, W.; Sham, L. J. *Phys. Rev.* **1965**, *140*, A1133.

(40) Parr, R. G.; Yang, W. *Density-Functional Theory of Atoms and Molecules*; Oxford University Press: New York, 1989.

(41) Kong, J.; White, C. A.; Krylov, A. I.; Sherrill, D.; Adamson, R. D.; Furlani, T. R.; Lee, M. S.; Lee, A. M.; Gwaltney, S. R.; Adams, T. R.; Ochsenfeld, C.; Gilbert, A. T. B.; Kedziora, G. S.; Rassolov, V. A.; Maurice, D. R.; Nair, N.; Shao, Y.; Basley, N. A.; Maslen, P. E.; Dombroski, J. P.; Daschel,

H.; Zhang, W.; Korambath, P. P.; Baker, J.; Byrd, E. F. C.; Van Voorhis, T.; Oumi, M.; Hirata, S.; Hsu, C.-P.; Ishikawa, N.; Florian, J.; Warshel, A.; Johnson, B. G.; Gill, P. M. W.; Head-Gordon, M.; Pople, J. A. *J. Comput. Chem.* **2000**, *21*, 1532.

(42) McDermott, G.; Prince, S. M.; Freer, A.; Hawthornwaite-Lawless, A. M.; Papiz, M. Z.; Cogdell, R. J.; Isaacs, N. W. *Nature* **1995**, *374*, 517.

(43) Hsu, C.-P.; Hirata, S.; Head-Gordon, M. *J. Phys. Chem. A* **2001**, *105*, 451.

(44) Hsu, C.-P.; Walla, P. J.; Head-Gordon, M.; Fleming, G. R. *J. Phys. Chem. B* **2001**, *105*, 11016.

Table 1. Comparison of the Energies of the 10 Lowest Singlet Excited States of the Full Phenylene-Linked ZnBC–BC Complex as Well as Of the Model Complex without the Phenylene Bridge with the Individually Calculated and Experimentally Determined Excitation Energies of the Q-States of the Monomers^a

state	ZnBC–BC complex			monomers	
	full	model	transition	calc.	expt.
1	1.33 (0.000)	1.32 (0.000)	ZnBC → BC CT		
2	1.46 (0.000)	1.47 (0.000)	BC → ZnBC CT		
3	1.86 (0.000)	1.90 (0.000)	BC → ZnBC CT		
4	1.94 (0.001)	1.96 (0.000)	ZnBC → BC CT		
5	2.05 (0.393)	2.07 (0.266)	π – π^* ZnBC (Q _x)	2.07 (0.231)	1.65 ⁴⁹
6	2.09 (0.131)	2.12 (0.170)	π – π^* BC (Q _x)	2.10 (0.187)	1.6 ⁵⁰
7	2.38 (0.059)	2.40 (0.038)	π – π^* BC (Q _y)	2.39 (0.034)	2.3 ⁵⁰
8	2.42 (0.019)	2.46 (0.018)	π – π^* ZnBC (Q _y)	2.44 (0.026)	2.2 ⁴⁹
9	2.43 (0.022)	2.42 (0.000)	ZnBC → BC CT		
10	2.58 (0.000)	2.66 (0.000)	BC → ZnBC CT		

^a The oscillator strength of each transition is given in brackets behind the corresponding energy. All calculations have been performed at the level of TDDFT/BLYP/6-31G*, and all energies are given in eV.

Table 2. The 12 Lowest Excited Singlet States of the Bacteriochlorophyll–Spheroidene Complex Calculated at the Level of TDA/BLYP/3-21G Are Given Together with the Results Obtained with the Hybrid Approach (See Section 2)^a

state	TDA/BLYP/3-21G energy (strength)	hybrid approach energy
Car-to-BChl CT	0.34 (0.000)	1.97
Car-to-BChl CT	0.98 (0.000)	
Car-to-BChl CT	1.52 (0.000)	
Car-to-BChl CT	1.57 (0.000)	
Car-to-BChl CT	1.65 (0.000)	
Car-to-BChl CT	1.67 (0.000)	
Q _y (BChl)	1.76 (0.007)	1.76
Car-to-BChl CT	1.94 (0.000)	
S ₁ (Spher)	1.95 (0.389)	1.95
Q _x (BChl)	1.98 (0.090)	1.98
BChl-to-Car CT	2.00 (0.000)	
S ₂ (Spher)	2.02 (1.131)	2.02

^a The strength of the states is given in brackets behind their energies (eV). The assignment of the states has been performed according to the molecular orbitals involved in the transition.

correct energetic order, which is not the case in either CIS or full TDDFT.^{19,44} Unfortunately, the use of larger basis sets is at present prohibitive due to the enormous size of the complex and the need to run a series of calculations. However, in previous calculations on chlorophyll–carotenoid complexes, it has been shown that TDA/TDDFT/BLYP/3-21G yields reasonable excitation energies for the lowest excitation energies of interest,¹⁹ and also here this is the case. The experimental values for the excitation energies of the Q_y, S₁, Q_x, and S₂ states of 1.6, 1.7, 2.1, and 2.4 eV,²⁸ respectively, are given in the correct order and within 0.1–0.2 eV error (Table 2). Only the S₂ state, which is of less relevance in this investigation, is underestimated by about 0.4 eV. The excited states have also been calculated along a distance coordinate between spheroidene and bacteriochlorophyll employing the hybrid TDDFT-CIS method to assess the error in the calculation of the CT states when only TDA/TDDFT is employed.

4. Results and Discussion

4.1. Charge-Transfer States in the Zincbacteriochlorin–Bacteriochlorin Complex. Weakly interacting complexes of tetrapyrroles, for example, porphyrins, chlorophylls, or chlorins and in this investigation zincbacteriochlorin–bacteriochlorin (ZnBC–BC) complexes, are important model systems for the investigation of the function of photosynthetic arrays of chlorophylls, which are present in light-harvesting complexes of plants and purple bacteria.^{23–25} A detailed understanding of the

molecular mechanisms of energy and electron-transfer processes in such simplified model complexes is crucial for the development of molecular mechanisms of photosynthetic processes. In turn, this requires reliable knowledge of the energetic position of the electronically excited states in these systems. Previous theoretical investigations of such model complexes by Yamaguchi et al.²² employing standard TDDFT identified low-lying charge-transfer (CT) excited states, which were calculated to be energetically well below the Q-states of the individual tetrapyrroles. This implies that, in oligomeric tetrapyrrol systems, the excited Q-states can, in principle, decay nonradiatively into the CT states. This process corresponds to electron-transfer quenching of the excited-state fluorescence. However, in recent experiments, no fluorescence quenching has been observed in such tetrapyrrol complexes.²⁴ In the following paragraphs, we will show that the energetically low-lying CT states are artifacts of the TDDFT calculations and that in reality these states are located well above the Q-states, and, as a consequence, electron-transfer quenching cannot occur.

The structure of the investigated phenylene-linked ZnBC–BC complex is depicted in Figure 2 and is characterized by the coplanar ZnBC and BC units which are linked via a phenylene ring which is perpendicular to the planes of the tetrapyrroles. The phenylene linkage exhibits a trans (1,4)-substitution pattern. Because of the perpendicular orientation of the π -system of the phenylene linkage to the π -systems of the ZnBC and BC ring, they do not overlap, and one can expect only a minor influence of the phenylene ring onto the energetically low-lying electronic π – π^* excitations of the complex which are located at the ZnBC or BC ring. This is further corroborated by a comparison of the geometrical parameters of the monomers with those of the phenylene-linked complex which reveals that the linkage has essentially no influence on them. The average difference between the bond lengths of the individually optimized monomers and the optimized complex is less than 0.001 Å. Overall, the obtained geometrical parameters at the level of DFT/B3LYP/6-31G* agree very favorably with theoretical values computed by Ghosh at the level of DFT employing a local xc-functional⁴⁵ as well as with crystallographic data on chlorins,⁴⁶ bacteriochlorins,⁴⁷ and isobacteriochlorins.⁴⁸ Because the explicit values of the geometrical parameters are only of minor interest in this context, the Cartesian coordinates of the optimized ZnBC, BC, and phenylene-linked ZnBC–BC complex are provided in the Supporting Information.

For comparison, the electronically excited singlet states of the monomers (zinc bacteriochlorin (ZnBC) and free-base bacteriochlorin (BC)) have been calculated employing TDDFT with the BLYP functional and the 6-31G* basis set. Our results are essentially identical to those obtained by Yamaguchi et al. who also used TDDFT in combination with the BLYP functional but with a slightly different basis set.²² At this level of theory, ZnBC possesses weakly allowed singlet excited states at 2.07 and 2.44 eV as well as strongly allowed transitions at 3.62 and 3.88 eV, which are interpreted as the well-known Q_x and Q_y as well as B_y and B_x states, respectively. The corresponding states

(45) Ghosh, A. *Acc. Chem. Res.* **1998**, *31*, 189.

(46) Strauss, S. H.; Silver, M. E.; Ibers, J. A. *J. Am. Chem. Soc.* **1983**, *105*, 4108.

(47) Barkigia, K. M.; Fajer, J.; Chang, C. K.; Young, R. *J. Am. Chem. Soc.* **1984**, *106*, 6457.

(48) Barkigia, K. M.; Fajer, J.; Chang, C. K.; Williams, G. J. B. *J. Am. Chem. Soc.* **1982**, *104*, 315.

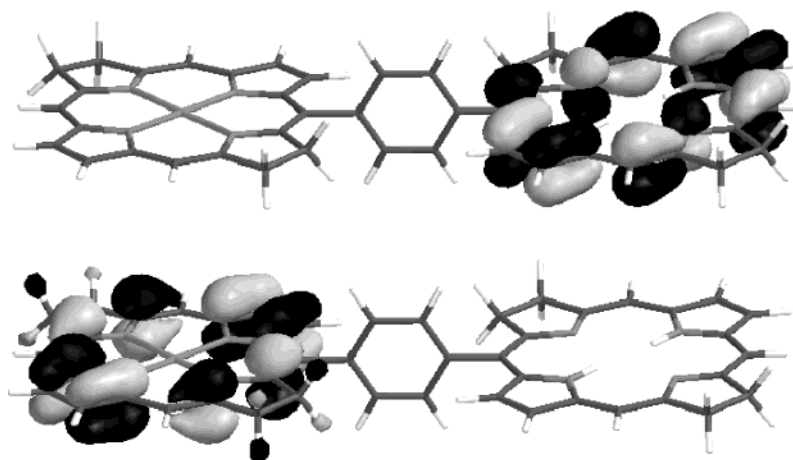


Figure 3. Highest occupied molecular orbital (HOMO, bottom) and lowest unoccupied molecular orbital (LUMO, top) of the ZnBC–BC complex. In the lowest excited CT state, an electron is transferred from the HOMO to the LUMO, and thus this transition corresponds to an electron transfer from ZnBC to BC.

of bacteriochlorin are found at energies of 2.10 (Q_x), 2.39 (Q_y), 3.67 (B_y), and 3.85 eV (B_x). Our calculated as well as experimental values^{49,50} for the excitation energies of the Q states are given in Table 1. All values are in reasonable agreement with other calculations of the electronic absorption spectra of ZnBC and BC.^{51–53}

Using the same theoretical approach for the calculation of the 10 lowest singlet excited states of the full (1,4)-phenylene-linked ZnBC–BC complex (Figure 2), one obtains the values given in Table 1. As expected, the Q-states of the constituting monomers are found at almost exactly identical energies in the linked complex. They are slightly red-shifted by only 0.01–0.02 eV. In addition to the monomer states, further energetically low-lying states are found at 1.33, 1.46, 1.86, and 1.94 eV. The energetically lowest state at 1.33 eV is a pure one-electron transition from the highest occupied molecular orbital (HOMO) into the lowest unoccupied molecular orbital (LUMO), and analysis of these MOs (Figure 3) clearly shows that this state corresponds to an electron transfer from ZnBC to BC. In analogy, states 2 and 3 at 1.46 and 1.86 eV represent BC-to-ZnBC CT states, while state 4 at 1.94 eV is again a ZnBC-to-BC CT state. Of course, these states cannot be present if the monomers are calculated individually, but are a characteristic of complex formation.

However, as pointed out in section 2, the calculated values of the CT states are given at too low energies, which easily can be confirmed by simple electrostatic considerations. Assuming that the separated charges in the CT states could be treated as point charges, the distance-dependent excitation energy of the energetically lowest ZnBC-to-BC CT state $\omega_{CT}(R)$ can simply be estimated via

$$\omega_{CT}(R) > IP_{ZnBC} + EA_{BC} - 1/R \quad (8)$$

where IP_{ZnBC} is the ionization potential of the ZnBC monomer,

- (49) Vasudevan, J.; Stibrany, R. T.; Bumby, J.; Knapp, S.; Potenza, J. A.; Emge, T. J.; Schugar, H. J. *J. Am. Chem. Soc.* **1996**, *118*, 11676.
 (50) Scheer, H.; Inhoffen, H. H. In *The Porphyrins*; Dolphin, D., Ed.; Academic: New York, 1978; Vol. 2, p 45.
 (51) Hasegawa, J.; Ozeki, Y.; Ohkawa, K.; Hada, M.; Nakatsuji, H. *J. Phys. Chem. B* **1998**, *102*, 1320.
 (52) Hashimoto, T.; Choe, Y. K.; Nakano, H.; Hirao, K. *J. Phys. Chem. A* **1999**, *103*, 1894.
 (53) Parusel, A. B. J.; Grimme, S. *J. Porphyrins Phthalocyanines* **2001**, *5*, 225.

EA_{BC} is the electron affinity of bacteriochlorin, and $1/R$ is the electrostatic attraction between them. Of course, R corresponds to the distance between the charges, which in our approximation is chosen to be the smallest distance between the carbon atoms of the different tetrapyrrol rings in the (1,4)-phenylene-linked ZnBC–BC complex, which has a value of 5.84 Å (see also Figure 2). At the level of DFT/BLYP/6-31G*, IP_{ZnBC} has a value of 5.57 eV and EA_{BC} is given as -0.42 eV, yielding an excitation energy for the lowest ZnBC-to-BC CT state of about 2.69 eV at the equilibrium distance R of the linked complex. In this equation, the cation and anion are treated as point charges and the shortest possible distance R is assumed, which of course leads to an overestimation of the electrostatic attraction. As a consequence, the estimated excitation energy ω_{CT} is a true lower bound to the correct value. Comparison with the excitation energy calculated at the level of TDDFT/BLYP/6-31G*, which has a value of 1.33 eV, yields a minimum error of 1.36 eV for this CT state. This demonstrates the tendency of TDDFT to underestimate the excitation energies of CT states drastically. It is worthwhile to note that the excitation energies of the CT states computed with TDDFT correspond in fact exactly to the difference of the orbital energies involved in the excitations, as we have already discussed in section 2. For instance, the excitation energy of the lowest CT state (1.33 eV) is solely given by the difference of the HOMO (-3.70 eV) and LUMO (-2.37 eV) energies of the electronic ground state.

As the next step, the dependence of the excitation energies of the lowest CT states on the distance R between the separated charges will be investigated. This requires the introduction of a suitable model complex, in which the distance between the positive and negative charges of the CT state can be easily varied. For the (1,4)-phenylene-linked ZnBC–BC complex, this is easily accomplished by neglecting the phenylene bridge, and choosing the distance between the formerly connected carbon atoms as the distance coordinate R , which has a value of 5.84 Å in the linked complex and was used previously to estimate the minimum excitation energy, ω_{CT} , in eq 8. As can be seen in Table 1, the phenylene bridge has only a minor influence on the 10 lowest excited states of the complex, which are slightly shifted by an average of 0.03 eV, while the largest shift of 0.08 eV occurred for state 10. As a consequence, the model complex

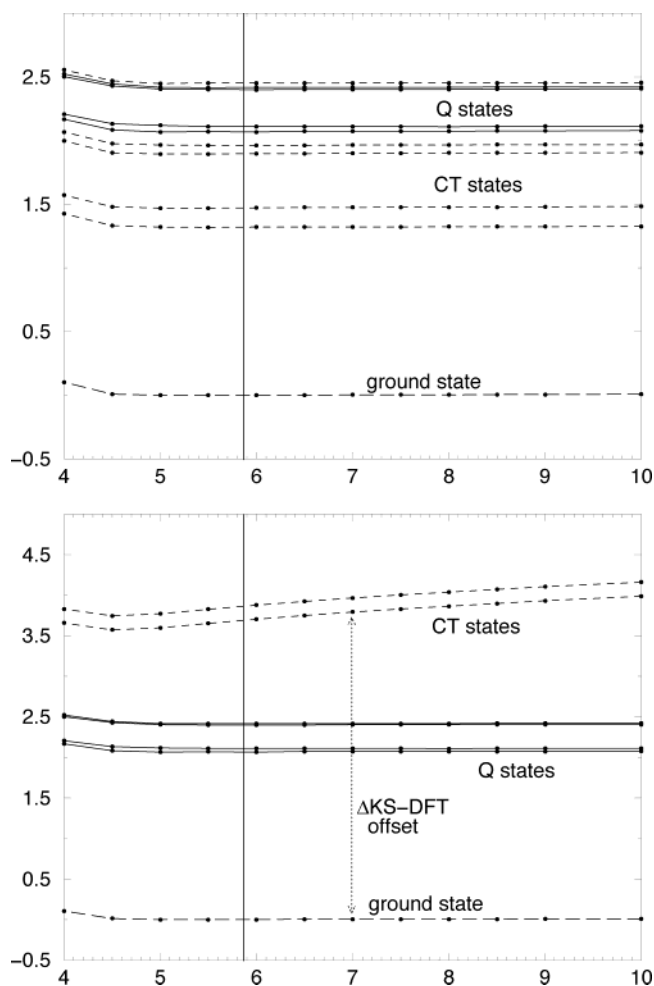


Figure 4. Potential energy curves of the lowest singlet excited states of the ZnBC–BC complex along the distance coordinate R calculated with TDDFT/BLYP/6-31G* (top) and with the hybrid approach (bottom, see section 2 for details). Short-dashed lines correspond to CT excited states, solid lines are the valence-excited Q states, and the long-dashed line represents the electronic ground state.

can be used in further calculations without losing the general validity of the obtained results.

To investigate the asymptotic behavior of the excited states and, in particular, of the excited CT states of the ZnBC–BC complex, the 10 lowest excited states of the model complex (Figure 2) have been calculated employing TDDFT with the BLYP functional and the 6-31G* basis set along the distance coordinate R . The obtained potential energy curves (PECs) are displayed in the upper part of Figure 4. As can be easily seen, the potential energy curves of the CT states are constant along the distance R between the monomers (the excitation energies correspond to the orbital energy differences), and they do not show the correct $1/R$ dependence. This is due to the electron-transfer self-interaction which is not canceled in the employed pure BLYP functional as we have outlined in section 2. In the lower part of Figure 4, the potential energy curves obtained with the proposed hybrid approach of TDDFT and CIS are shown. In this figure, the electron-transfer self-interaction free PECs of the two energetically lowest CT states have been calculated along the distance coordinate R with CIS and shifted by a Δ DFT offset. This offset has been calculated for the lowest ZnBC-to-BC CT state to be 3.79 eV and for the lowest BC-

to-ZnBC CT state to be 3.95 eV at the level of BLYP/6-31G*. These curves are then plotted together with the curves of the Q-states given by the TDDFT/BLYP/6-31G* calculation. The obtained picture is substantially different from that obtained by TDDFT alone. First, the two energetically lowest CT states are clearly above the valence-excited Q-states of the complex. Second, the CT states do exhibit the correct asymptotic behavior such that the excitation energies do increase with $1/R$. Furthermore, from this picture, one can obtain a reasonable value for the lowest intramolecular CT states of the 1,4-phenylene-linked ZnBC–BC complex. At the value of 5.84 Å, the value of R in the full complex, the lowest CT states possess an excitation energy of 3.75 eV and the second lowest CT state has an excitation energy of 3.91 eV, which agrees with the previously computed lower bound for the excitation energies of these states. As compared to the TDDFT computed values of 1.33 and 1.46 eV for these states, this yields errors in the TDDFT calculation of 2.42 and 2.43 eV, respectively. As a consequence, the spectrum as obtained by TDDFT alone and published previously²² is an artifact of the approximate xc-functionals employed in present-day TDDFT.

The different results for the CT states obtained either with TDDFT alone or with the qualitatively correct hybrid approach lead to different spectroscopic predictions and interpretations. The upper part of Figure 4, the erroneous results of the TDDFT calculation, suggest that significant fluorescence quenching through nonradiative decay into the energetically low-lying CT states should be observed when the Q-states of the linked ZnBC–BC complex are excited. Yet, in fact, no fluorescence quenching is experimentally observed in porphyrin dimer systems.²⁴ On the other hand, this is corroborated by the qualitatively correct curves obtained with the hybrid approach (lower part of Figure 4), which show that fluorescence quenching of the Q-states cannot occur because the CT states are energetically well above the otherwise lowest Q-states. Thus, the findings with the suggested hybrid approach are in agreement with the experimental observation.

4.2. Charge-Transfer States in the Bacteriochlorophyll–Spheroidene Complex. In a recent elaborate experimental investigation of the LH2 complex of *Rhodobacter sphaeroides* with femtosecond absorption spectroscopy, the formation of a spheroidene (Spher) radical cation has been observed upon excitation of its S_2 state.²⁸ The formation of the radical cation indicates that one possible decay mechanism of the S_2 excitation energy in the LH2 complex is via electron transfer from Spher to bacteriochlorophyll (BChl). To corroborate this possibility, theoretical calculations were also performed for a B800' BChl–Spher complex at the level of TDDFT employing the B3LYP functional and 6-31G* basis set²⁸ (Figure 5). Several Spher-to-BChl CT states have been obtained which are energetically lower than the S_2 state of Spher, thus allowing for electron-transfer quenching of the originally excited S_2 state. Although this is in agreement with the experiments, we have shown in the previous sections that TDDFT generally underestimates the excitation energies of CT excited states and, therefore, the results of the TDDFT calculations need to be reconsidered.

In analogy to the previous calculation, we also use the reoptimized crystal structure of the B800' BChl–Spher complex (Figure 5) of *Rhodospseudomonas acidophila*.⁴² The reoptimization is described in detail in section 3.2. The obtained

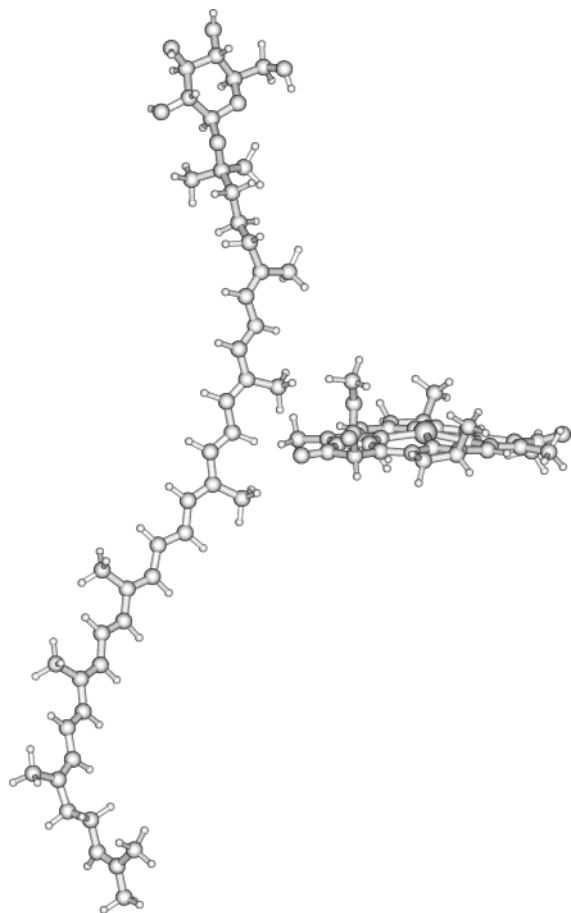


Figure 5. Structure of the B800' bacteriochlorophyll–spheroidene complex.

geometrical parameters for the bond lengths and angles of BChl and Spher agree with typical values, and, in particular, the conjugated carbon chain of spheroidene exhibits the typical bond length alternation pattern of single and double bonds. The electronically excited singlet states of the BChl–Spher complex have been calculated using TDA/BLYP/3-21G. In agreement with the calculations of Polivka et al.,²⁸ a manifold of energetically low-lying charge-transfer excited states were found (Table 2). As we have shown in section 2, the excitation energies of the CT states are drastically underestimated, because they suffer from self-interaction. Furthermore, the potential energy curves of the CT excited states calculated along the distance coordinate R also do not exhibit the correct $1/R$ asymptote. The distance coordinate R is defined as the distance between the ring carbonyl group of BChl and the spatially closest hydrogen atom of Spher as depicted in Figure 6.

To obtain a more reliable estimate for the excitation energy of the energetically lowest CT state, we employed again the proposed hybrid approach consisting of TDA/BLYP and CIS, and we recalculated the excited states along the intermolecular distance coordinate R . The obtained potential energy curves are shown in Figure 7. While the curves for the valence-excited states, Q_y and Q_x of BChl and S_1 and S_2 of Spher, have been calculated using TDA/BLYP alone, the curve of the energetically lowest excited CT state has been obtained by employing CIS and shifting the curve by the Δ DFT value of 2.787 calculated with DFT/BLYP/3-21G. In this qualitatively correct picture, the potential energy curve of the CT state does exhibit

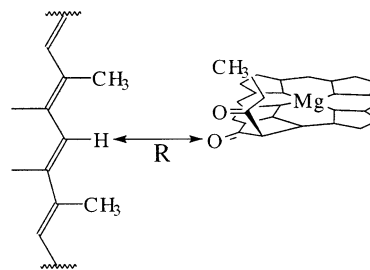


Figure 6. The distance coordinate R in the BChl–Spher complex is defined as the distance between the ring carbonyl group and the spatially closest hydrogen atom of spheroidene. In the crystal structure, this distance R has a value of 2.26 Å.

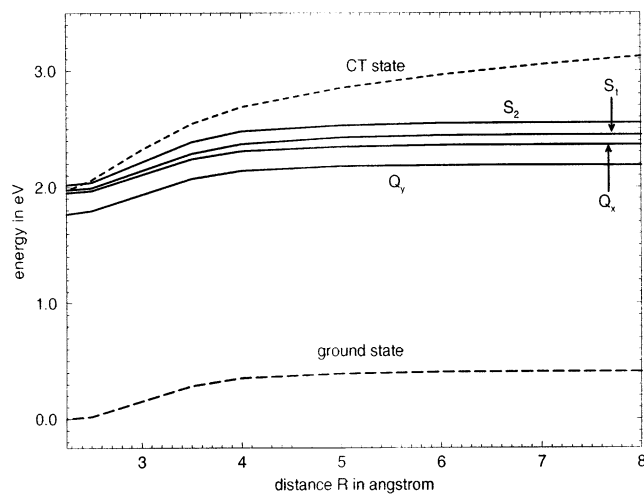


Figure 7. Potential energy curves of the lowest singlet excited states of the BChl–Spher complex along the intermolecular distance coordinate R . The hybrid TDA/CIS approach (see section 2 for details) has been applied. The dashed line corresponds to the energetically lowest CT states, solid lines represent valence-excited states, and the long-dashed line is the electronic ground state.

the physically correct $1/R$ asymptote. Furthermore, as one can easily see from Figure 7, the energetically lowest CT state is higher in energy than the valence-excited states Q_y , Q_x , S_1 , and S_2 at distances larger than about 2.5 Å. Only at distances shorter than 2.5 Å does the CT state drop energetically below the S_2 state and can it be energetically populated after laser excitation of the S_2 state. At the equilibrium distance of $R = 2.26$ Å, this is the case, because the S_2 state has a vertical excitation energy of 2.02 eV, while the CT state is at 1.97 eV. A similar situation has been found when xanthophyll–chlorophyll complexes were studied with the hybrid approach.^{6,19} Comparison of the excitation energy obtained with the hybrid approach with that given by TDA alone indicates an error of about 1.6 eV for the latter number. This demonstrates once more how severe the failure of TDDFT and TDA for CT excited states can be.

In summary, our calculations corroborate the experimental findings by Polivka et al.,²⁸ because according to our results electron-transfer quenching should be possible for the S_2 excited state of Spher. However, the involved energy differences of about 0.1 eV are very small and may well be beyond the accuracy of TDDFT or the applied hybrid approach. Thus further, more elaborate, quantum chemical studies are probably necessary to yield quantitative numbers. Unfortunately, such studies are at present still beyond the capacity of modern computers. Nevertheless, the results obtained with the hybrid

approach certainly reflect the true picture more closely than the results given by TDDFT or TDA alone.

Finally, we have performed gas-phase calculations, while the experiments were performed in the protein environment of LH2. This will have of course a distinct influence on the excited states which is in detail not known, but generally one can expect that the CT excited states are strongly stabilized in a polar medium due to their gigantic dipole moment. For instance, the calculated static dipole moment of the lowest CT state of the BChl–Spher complex at the distance $R = 2.26 \text{ \AA}$ has a value of 81 D, while its electronic ground state has a dipole moment of only 4.7 D. Therefore, the excitation energy of the lowest CT state drops further in energy as compared to the other valence-excited state in the protein and can, in principle, be populated in the described experiment upon laser excitation of the S_2 state of spheroidene.

5. Summary and Conclusions

Time-dependent density functional theory (TDDFT) is a very popular approach for calculating electronic excitation spectra and has been applied to various molecular systems. It is especially well suited to study large systems, because its computational cost is relatively low as compared to other correlated quantum chemical approaches. Although TDDFT is a formally exact method, one introduces errors by using approximate xc-functionals, which leads to problems in the description of, for instance, Rydberg states, large π -systems, or charge-transfer excited states. Here, we explored the failure of TDDFT to yield reasonable excitation energies for CT states as well as to give the correct $1/R$ asymptotic behavior of CT excited states with respect to a distance coordinate R between the separated charges, when standard xc-functionals (SVWN, BLYP, B3LYP, etc.) are employed.

The error in the excitation energies of CT excited states can be traced back to the self-interaction error present in the orbital energies of the DFT calculation, which leads to an underestimation of the HOMO–LUMO gap. The incorrect asymptotic behavior of the CT excited states is also due to a self-interaction problem, which we term electron-transfer self-interaction. It originates from the fact that the orbital energy of the electron-accepting orbital contains the Coulomb repulsion between the accepting and the donating orbital, which is not present in the CT state but which is not correctly canceled in the TDDFT calculation unless exact exchange is present. Furthermore, a hybrid approach is presented which consists of a combination of TDDFT for valence-excited states and CIS in combination with Δ DFT for the lowest CT state. This approach represents a practical way of circumventing the electron-transfer self-interaction problem and of yielding asymptotically correct potential energy curves and reasonable estimates of the excitation energy of CT states in large molecular systems.

Despite these failures of TDDFT, it has been applied to large molecular systems in which inter- or intramolecular CT states might play important roles. Here, we have chosen two examples: a (1,4)-phenylene-linked zincbacteriochlorin–bac-

teriochlorin (ZnBC–BC) complex and a bacteriochlorophyll–spheroidene (BChl–Spher) complex, which have both been theoretically investigated previously employing TDDFT. In both systems, spurious energetically low-lying excited CT states have been identified using TDDFT alone, and application of the qualitatively correct hybrid approach shows that the excitation energies of the lowest CT states are drastically underestimated by TDDFT by 2.4 and 1.6 eV in the ZnBC–BC and BChl–Spher complexes, respectively.

Our calculations for the (1,4)-phenylene-linked ZnBC–BC complex demonstrate that CT excited states are energetically well above the valence-excited Q states and thus are not relevant for the photochemistry of the ZnBC–BC complex in this energy regime. In the case of the BChl–Spher complex, however, the energetically lowest Spher-to-BChl CT state is in the energy regime of the relevant valence-excited states (Q_y and Q_x of BChl and S_1 and S_2 of Spher) and needs to be considered when energy-transfer or electron-transfer processes in this or similar systems are discussed.

Because intermolecular and intramolecular CT states are ubiquitous, for example, in weakly interacting molecular complexes of all sizes, large molecules with subgroups of different local electron affinities, or in solutions and solids, TDDFT calculations must be performed with great caution for such systems. Especially, in condensed phases a manifold of spurious CT states can be expected to occur within the framework of TDDFT employing standard xc-functionals. Spurious CT states must be eliminated by careful inspection of the nature of the excited states, and the excitation energies of the valence-excited states of interest should be, if possible, checked against experimental values or benchmark calculations. In the present form, however, employing standard xc-functionals, TDDFT is not a black-box method for medium-sized and large molecules, but requires experience and knowledge of the investigated molecular system to lead to correct results.

Acknowledgment. Stimulating discussions with Prof. A. Görling, Prof. E. K. U. Gross, Dr. G. K.-L. Chan, and T. Dutoi are gratefully acknowledged. A.D. is financially supported by the Deutsche Forschungsgemeinschaft as an “Emmy-Noether” fellow. This work was also supported by the Director, Office of Energy Research, Office of Basic Energy Sciences, Chemical Science Division of the U.S. Department of Energy under Contract No. DE-AC03-76SF00098. Computer time has been generously provided by the National Energy Research Scientific Computing Center (NERSC).

Supporting Information Available: Cartesian coordinates of the optimized structures of the phenylene-linked zincchlorin–chlorin complex as well as of the separately optimized individual molecules zincchlorin and chlorin; Cartesian coordinates of the reoptimized structure of the bacteriochlorophyll–spheroidene complex (PDF). This material is available free of charge via the Internet at <http://pubs.acs.org>.

JA039556N